Published in final edited form as:
Wound Repair Regen. 2010 ; 18(6): 586–593. doi:10.1111/j.1524-475X.2010.00632.x.

Accelerated Wound Healing Mediated by Activation of Toll-like Receptor 9

Takashi Sato, MD, PhD[1,2], **Masaki Yamamoto, MD**[1], **Takeshi Shimosato, MD, PhD**[1], and **Dennis M. Klinman, MD, PhD**[1]

[1]Cancer and Inflammation Program, National Cancer Institute, Frederick, MD 21702

Abstract

Wound healing is mediated through complex interactions between circulating immune cells and local epithelial and endothelial cells. Elements of the innate immune system are triggered when Toll like receptors (TLR) are stimulated by their cognate ligands, and previous studies suggest that such interactions can accelerate wound healing. This work examines the effect of treating excisional skin biopsies with immunostimulatory CpG oligodeoxynucleotides (ODN) that trigger via TLR9. Results indicate that CpG (but not control) ODN accelerate wound closure and reduce the total wound area exposed over time by >40% ($p < 0.01$). TLR9 KO mice, a strain unresponsive to the immunomodulatory effects of CpG stimulation, are unresponsive to ODN treatment and exhibit a general delay in healing when compared to wild type mice. CpG ODN administration promoted the influx of macrophages to the wound site and increased the production of vascular endothelial growth factor (VEGF), expediting neovascularization of the wound bed ($p < 0.01$ for both parameters). Stimulation via TLR9 thus represents a novel strategy to accelerate wound healing.

Keywords

CpG oligonucleotide; wound healing; TLR9; VEGF

INTRODUCTION

Wound healing is a multi-step process that culminates in the regeneration of normal dermal and epidermal tissue. The first stage in this process is marked by an inflammatory response in which neutrophils and macrophages infiltrate the wound site. This is followed by a proliferative phase marked by revascularization and the formation of granulation tissue (1). These events are influenced by growth factors (such as VEGF) and cytokines secreted by inflammatory and epithelial cells situated at the edges of the wound (2-5).

Recent reports indicate that the innate immune system can influence the speed at which a wound heals. For example, activation via TLR4 accelerates wound repair by improving epithelial cell migration and VEGF production, while disruption of the MyD88 dependent TLR signaling pathway slows healing (6). Studies performed in mice and humans show that

Corresponding author (to whom reprints should be addressed): Dennis M. Klinman, Bldg 567 Rm 205 NCI in Frederick, Frederick, MD 21702, (W) 301 228 4265, (F) 301 228 4281, klinmand@mail.nih.gov.
[2]Current Address: Department of Internal Medicine and Clinical Immunology, Yokohama City, University Graduate School of Medicine, Yokohama, Japan

CONFLICT OF INTEREST

Dr. Klinman and members of his lab hold or have applied for patents concerning the activity of CpG ODN, including their use in accelerating wound repair. The rights to all such patents have been transferred to the US government.

synthetic oligodeoxynucleotides (ODN) expressing unmethylated CpG motifs (patterned after immunostimulatory sequences present in bacterial DNA) trigger the innate immune system via TLR9 (7-12). Of relevance to studies of wound healing, CpG ODN have been used safely in humans (13-15), and induce an inflammatory response that includes the production of VEGF (16-18).

This work examines the effect of local CpG ODN administration on the healing of full-thickness excisional skin biopsies. Wound closure was significantly accelerated when normal mice were treated with CpG but not control ODN. No such effect was observed in TLR9 KO mice (a strain unresponsive to CpG stimulation). Several findings suggest that VEGF plays a critical role in this process. VEGF levels are significantly elevated following CpG ODN treatment, and wound healing delayed by the addition of neutralizing anti-VEGF Abs. Moreover, CpG ODN promote the migration of macrophages to the wound site and stimulate them to secrete VEGF. As CpG ODN have been safely administered to humans, current findings suggest that immunostimulatory oligonucleotides may provide a novel, inexpensive, safe and effective means of improving wound repair.

MATERIALS AND METHODS

Mice and reagents

Specific pathogen free female BALB/c mice and congenic TLR 9 KO mice (kind gift of Dr. Shizuo Akira, Osaka, Japan) were maintained in the NCI specific pathogen free animal facility (Frederick, MD). Animals were housed in sterile microisolator cages in a barrier environment, and studied at 12 wk of age. All experiments were conducted using ACUC approved protocols.

CpG ODN 1555; GCTAGACGTTAGCGT and control ODN 1612; GCTAGAGCTTAGCGT were used in all studies (19). All ODNs were synthesized at the Center for Biologics Core Facility and were free of endotoxin and protein contamination. ODN concentration was monitored by NanoDrop Spectrophotometry (Thermo Fisher Scientific, DE). The release of ODN from BME was calculated by the formula: (CpG concentration in the lower chamber) × (volume of both chambers) / (initial CpG concentration in the upper chamber) (volume of BME) × 100%. Results were derived from 3 independent experiments.

Other reagents used include: rabbit anti-mouse VEGF A165 and anti-CD31 Abs, rat anti-mouse F4/80 Ab, rabbit polyclonal IgG and rat IgG2b (all from Abcam, Cambridge MA), Alexa Fluor 594 goat anti-rabbit IgG and Alexa Fluor 488 goat anti-rat IgG (Molecular Probes, Inc, Eugene OR). Growth factor reduced basement membrane extract (BME) without phenol red was purchased from Trevigen (Gaithersburg, MD).

Cell preparation

Peritoneal macrophages were isolated from mice injected intraperitoneally with 3% thioglycolate as previously described (20). Cells were maintained in RPMI 1640 supplemented with 10% FCS, 100 U/ml penicillin, 100 μg/ml streptomycin, 25 mM HEPES, 1 mM sodium pyruvate, 0.1 mM non essential amino acids, and 0.0035% 2 ME.

In vitro VEGF assay—Peritoneal macrophages were seeded into the upper chamber of a transwell plate at 5×10^5 cells/well and incubated for up to 120 hr. Medium in the upper chamber was replaced with BME plus ODN. VEGF levels in the lower chamber were measured using a commercial ELISA kit (R&D Systems, Minneapolis, MN) as

recommended by the manufacturer. All values were corrected for background VEGF levels in wells containing BME but no cells.

In vivo wound repair model—The wound repair model of Devalarja et al was used to analyze the effects of CpG ODN in vivo (6,21,22). In brief, mice were anesthetized by intraperitoneal injection of ketamine (80 mg/kg) plus xylazine (10 mg/kg) (21). The skin on the back was cleaned, shaved, and sterilized with betadine solution followed by 70% ethanol. A 6 mm full thickness (including the Pannilulus carnosus) excisional punch biopsy (Acu Punch, Fort Lauderdale, FL) was taken from the right and left upper paravertebral region of each animal (22). Individual biopsy sites were coated with liquid BME ± 50 μg of ODN (an amount selected on the basis of preliminary dose-ranging studies), and allowed to gel over 15 min. After gelling, the biopsy sites were separated by a strip of Vaseline ointment (to prevent cross contamination of ODN) and covered with non-adhesive sterile gauze. Mice were wrapped with a form-fitting bandage to further protect the biopsy sites. In one series of experiments, mice were injected i.p. with 10 μg of neutralizing goat anti mouse VEGF Ab (R&D Systems, Minneapolis, MN) twice weekly starting 1 wk before biopsy.

Wounds were checked daily for infection at which time they were digitally photographed using an IX50 inverted microscope (Olympus, Center Valley, PA). Changes in wound contraction over time were calculated using NIH Image J software (Ver 1.37). Each treatment was tested and results averaged in a minimum of 6 independent animals/group.

Histopathological analysis

Biopsy sites were surgically removed, fixed in 10% formalin, and embedded in paraffin. Sections were stained with H&E for histological analysis. Immunohistochemical studies were performed as described previously (6,22,23). Briefly, de-waxed paraffin sections were antigen retrieved in 10 mM citrate buffer (pH 6.0) for 15 min and incubated with 10% normal serum (Nichirei, Tokyo, Japan) for 15 min at 37° C. Sections were stained with anti-VEGF or anti-CD31 (diluted 1:250) overnight at 4° C, or anti-F4/80 (diluted 1:50) for 1 hr at RT, washed, and treated with an alkaline phosphatase labeled universal immunoenzyme polymer (Nichirei, Tokyo, Japan) and visualized colorimetrically (Nichirei). To monitor the co-localization of VEGF and F4/80, sections were incubated with a combination of anti-VEGF and anti-F4/80 followed by fluorochrome-conjugated secondary antibodies at RT for 30 min. The sections were observed by fluorescence microscope (BZ-9000, Keyence, Osaka, Japan). Nuclei were counterstained with Meyer Hematoxylin (Nichirei) for colorimetrical analysis or with DAPI (Molecular probe) for fluorescence analysis. Areas of neovascularization (defined by CD31 binding) were measured and expressed as a percentage of the entire wound bed area. For morphometric analysis of wound sites, the distance between the migration tongues (δMT, see arrows in Fig 3) and area of granulation tissue (see “G” in Fig 3) were determined on fixed stained tissue as previously described (24).

Statistical analysis

Statistical analyses was performed using MedCalc, version 9.3.7.0 (MedCalc Software, Belgium). Differences between biopsy sites were assessed using two way analysis of variance (ANOVA). Changes in wound size were calculated as the area under the curve using serial measurements. All tests were two sided; probability values less than 0.05 were considered significant. All values are expressed as means ± SE unless otherwise noted.

RESULTS

CpG ODN treatment accelerates wound repair

Agents used to promote wound repair must be delivered to and persist at the injury site. Preliminary studies were performed to identify a formulation into which CpG ODN could be incorporated and then slowly released after topical administration. Results showed that CpG ODN mixed with liquid basement membrane extract (BME) gelled to form a protective barrier when applied to the skin (25-27). The release of CpG ODN from BME was monitored *in vitro* using a transwell system which showed that half of the incorporated ODN was released over the first 12 hr and the remainder over the following 2 – 3 days (Fig 1).

The effect of administering CpG-containing BME *in vivo* was examined using a well established murine model of wound healing (24). Two identical full thickness skin biopsies were taken from the right and left subscapular regions of individual mice. One site was treated with BME alone and the other with BME + CpG or control ODN. Sequential photographs provided a permanent record of the speed of wound closure.

Untreated biopsy sites and sites treated with BME ± control ODN healed at nearly identical rates (Fig 2 A,B). Biopsy sites treated with BME + CpG ODN healed significantly more rapidly, with 50% wound closure being achieved after 4.0 ± 1.1 vs 7.2 ± 0.9 days (44% faster, $p < 0.001$, Fig 2). Treatment with BME + CpG ODN reduced the total wound area exposed over time by >40% ($p < 0.001$, Fig 2).

To determine whether these effects required stimulation via TLR9 (the cognate receptor for unmethylated CpG motifs (10)), the studies were repeated in TLR9 KO mice. Wound closure in TLR9 KO animals was significantly delayed when compared to congenic BALB/c mice (50% healing at 9.3 ± 1.3 vs 7.2 ± 0.9 days, $p < 0.001$, Fig 2 C,D). Of greater importance, CpG ODN treatment had no effect on the rate of wound closure in TLR9 KO mice (Fig 2 C,D). These findings indicate that CpG-induced acceleration of wound healing is mediated in a TLR9-specific manner (10,28).

CpG ODN accelerate wound healing by promoting VEGF production

Biopsy sites were examined histologically on day 4 (the time point when macroscopic differences between treatment groups was greatest) to clarify the mechanism by which CpG ODN accelerated wound healing. Two histologic measures of healing were examined: the formation of granulation tissue and the magnitude of re-epithelialization. By both measures, there was a significant acceleration in the healing of biopsies from normal mice treated with BME + CpG ODN ($p < 0.05$, Fig 3 B,C). No such acceleration was observed in the TLR9 KO mice.

A clue to the mechanism underlying this effect arose in studies of new blood vessel formation (characterized by an influx of $CD31^+$ endothelial cells). As seen in Fig 4, CpG ODN treated biopsies of normal mice were characterized by the accelerated appearance of $CD31^+$ cells and increased new blood vessel formation ($p < 0.01$, Day 4). In contrast, neovascularization of TLR9 KO mice was significantly slower than in congenic BALB/c's, and was not increased by treatment with CpG ODN (Fig 4B).

While multiple factors might contribute to the observed acceleration in blood vessel formation, previous studies showed that CpG ODN could promote the production of the pro-angiogenic protein VEGF (16). Consistent with that finding, the number of cells producing VEGF was significantly increased by treatment with CpG (but not control) ODN ($p < 0.01$), an effect observed in BALB/c but not TLR9 KO mice (Fig 5). To determine whether this local production of VEGF might account for the increased blood vessel formation observed

after CpG ODN administration, neutralizing Ab was used to block the effect of locally produced VEGF. Co-administering anti-VEGF Ab with CpG ODN reduced the rate of wound closure by >80% ($p < 0.01$, Fig 6), falling to a level indistinguishable from that of wounds treated with anti-VEGF plus BME alone.

To clarify the cellular source of this CpG-induced VEGF, the phenotype of inflammatory cells at the wound site was examined. Previous studies established that macrophages enter sites of tissue injury where they facilitate angiogenesis and promote wound repair (6,29). As seen in Fig 7, treatment with CpG ODN further increased the frequency of macrophages at biopsy sites (characterized by the accumulation of F4/80-positive cells) ($p. < 0.01$). Since murine macrophages express TLR9 (30), the effect CpG ODN on VEGF production was examined. Individual histologic sections were double-stained to determine the phenotype of the VEGF-secreting cells. Results showed that a majority of the cells producing VEGF were $F4/80^{+}$ macrophages (Fig 8 A,B). Consistent with that conclusion, the secretion of VEGF by freshly isolated peritoneal macrophages was significantly increased by the addition of CpG ODN *in vitro* (Fig 8 C, $p < 0.01$).

DISCUSSION

Wound repair proceeds in multiple stages that include inflammation, re-vascularization and epithelial cell migration/proliferation (1). Current findings indicate that topical application of CpG ODN promotes the TLR9-dependent accumulation of macrophages at sites of tissue injury, stimulating local production of VEGF, and accelerating neovascularization and wound closure.

The activity of CpG ODN was monitored in vivo by preparing two full thickness skin biopsies on opposite sides of each animal (1,31,32). These sites were randomly treated with CpG or control ODN formulated in BME (which released the ODN in bioactive form over several days, Fig 1). Preliminary studies established the optimal dose and frequency of treatment. As seen in Fig 2, wound sites treated with CpG ODN healed significantly faster than sites treated with BME ± control ODN ($p < 0.01$). The time to 50% wound closure was reduced by 44% while the total wound area exposed over time was reduced by 41%.

Although multiple mechanisms might account for the observed acceleration in wound healing, immunohistochemical analysis showed that topical application of CpG ODN significantly increased local VEGF production and neovascularization ($p < 0.01$, Figs 4,5). This corresponded to a significant increase in the number of VEGF secreting macrophages at CpG-treated sites (Fig 7), a finding consistent with earlier studies showing that CpG ODN promoted VEGF production (33). The contribution of VEGF to CpG dependent wound healing was clarified by treating biopsy sites with anti-VEGF Ab. When VEGF was neutralized, the healing rate of sites treated with CpG ODN did not differ from controls (Fig 6). Additional study showed that CpG ODN treatment significantly increased the frequency of macrophages infiltrating the wound site, and that macrophages respond to CpG stimulation by producing VEGF (Figs 5,7 and 8) (16,36).

Several findings indicate that CpG-mediated wound closure was sequence-specific and TLR9-dependent. First, would healing in normal mice was accelerated by treatment with CpG but not control ODN (Fig 2 A,B). Second, CpG ODN did not accelerate healing TLR9 KO mice (Fig 2 C,D), indicating that the interaction of CpG DNA with its cognate TLR9 receptor underlies this beneficial effect. Of interest, the kinetics of wound healing in the TLR9 KO mice was delayed when compared to congenic controls, suggesting that this activation pathway may contribute physiologically to wound healing (perhaps through exposure to bacterial DNA in the gut or on the skin). This is consistent with previous studies

showing that optimal wound repair requires an intact MyD88 signaling cascade and that activation of the innate immune system via TLR4 can accelerate wound repair (6).

In summary, this work is the first to demonstrate that wound healing is significantly accelerated by local administration of CpG ODN. This effect is temporally associated with a CpG-dependent increase in VEGF production that enhances neovascularization. CpG ODN at doses exceeding 1 mg/Kg have been safely administered in human clinical trials, suggesting that topical administration of the much lower doses of ODN used in this work should be well tolerated (13,14,35-37). In toto, these findings suggest that CpG ODN may represent a safe and novel strategy to promote wound healing.

Acknowledgments

The assertions herein are the private ones of the authors and are not to be construed as official or as reflecting the views of the NIH or NCI at large.

This work was supported in part by grants from the Ministry of Education, Culture, Sports, Science and Technology of Japan (21790778) and from the Kanagawa Nanbyo Foundation.

REFERENCES

1. Singer AJ, Clark RA. Cutaneous wound healing. N Engl J Med. 1999; 341(10):738–46. [PubMed: 10471461]
2. Coussens LM, Werb Z. Inflammation and cancer. Nature. 2002; 420(6917):860–7. [PubMed: 12490959]
3. Werner S, Grose R. Regulation of wound healing by growth factors and cytokines. Physiol Rev. 2003; 83(3):835–70. [PubMed: 12843410]
4. Hoeben A, Landuyt B, Highley MS, Wildiers H, Van Oosterom AT, De Bruijn EA. Vascular endothelial growth factor and angiogenesis. Pharmacol Rev. 2004; 56(4):549–80. [PubMed: 15602010]
5. Frantz S, Vincent KA, Feron O, Kelly RA. Innate immunity and angiogenesis. Circ Res. 2005; 96(1):15–26. [PubMed: 15637304]
6. Macedo L, Pinhal-Enfield G, Alshits V, Elson G, Cronstein BN, Leibovich SJ. Wound healing is impaired in MyD88-deficient mice: a role for MyD88 in the regulation of wound healing by adenosine A2A receptors. Am J Pathol. 2007; 171(6):1774–88. [PubMed: 17974599]
7. Krieg AM, Yi A, Matson S, Waldschmidt TJ, Bishop GA, Teasdale R, Koretzky GA, Klinman DM. CpG motifs in bacterial DNA trigger direct B-cell activation. Nature. 1995; 374:546–8. [PubMed: 7700380]
8. Klinman DM, Yi A, Beaucage SL, Conover J, Krieg AM. CpG motifs expressed by bacterial DNA rapidly induce lymphocytes to secrete IL-6, IL-12 and IFNg. Proc Natl Acad Sci USA. 1996; 93:2879–83. [PubMed: 8610135]
9. Wagner H. Bacterial CpG-DNA activates immune cells to signal “infectious danger”. Adv Immunol. 1999; 73:329–68. [PubMed: 10399010]
10. Hemmi H, Takeuchi O, Kawai T, Sato S, Sanjo H, Matsumoto M, Hoshino K, Wagner H, Takeda K, Akira S. A Toll-like receptor recognizes bacterial DNA. Nature. 2000; 408:740–5. [PubMed: 11130078]
11. Takeshita F, Leifer CA, Gursel I, Ishii K, Takeshita S, Gursel M, Klinman DM. Cutting Edge: role of toll-like receptor 9 in CpG DNA-induced activation of human cells. J Immunol. 2001; 167(7): 3555–8. [PubMed: 11564765]
12. Klinman DM. Immunotherapeutic uses of CpG oligodeoxynucleotides. Nat Rev Immunol. 2004; 4(4):249–58. [PubMed: 15057783]
13. Halperin SA, Van Nest G, Smith B, Abtahi S, Whiley H, Eiden JJ. A phase I study of the safety and immunogenicity of recombinant hepatitis B surface antigen co-administered with an immunostimulatory phosphorothioate oligonucleotide adjuvant. Vaccine. 2003; 21(19-20):2461–7. [PubMed: 12744879]

14. Rynkiewicz D, Rathkopf M, Ransom J, Sim I, Giri L, Quinn J, Waytes T, Al-Adhami M, Johnson W, Nielsen C. Marked enhancement of antibody response to anthrax vaccine adsorbed with CpG 7909 in healthy volunteers. ICAAC. 2005 abstract LB-25.
15. Vollmer J, Krieg AM. Immunotherapeutic applications of CpG oligodeoxynucleotide TLR9 agonists. Adv Drug Deliv Rev. 2009; 61(3):195–204. [PubMed: 19211030]
16. Zheng M, Klinman DM, Gierynska M, Rouse BT. DNA containing CpG motifs induces angiogenesis. Proc Natl Acad Sci U S A. 2002; 99(13):8944–9. [PubMed: 12060721]
17. Pinhal-Enfield G, Ramanathan M, Hasko G, Vogel SN, Salzman AL, Boons GJ, Leibovich SJ. An angiogenic switch in macrophages involving synergy between Toll-like receptors 2, 4, 7, and 9 and adenosine A(2A) receptors. Am J Pathol. 2003; 163(2):711–21. [PubMed: 12875990]
18. Fujimoto C, Klinman DM, Shi G, yin H, Vistica BP, Lovaas JD, Wawrousek EF, Igarashi T, Chan CC, Gery I. A suppressive oligodeoxynucleotide inhibits ocular inflammation. Clin Exp Immunol. 2009; 156(3):528–34. [PubMed: 19438607]
19. Tross D, Klinman DM. Effect of CpG oligonucleotides on vaccine-induced B cell memory. J Immunol. 2008; 181(8):5785–90. [PubMed: 18832738]
20. Sato T, Shimosato T, Alvord WG, Klinman DM. Suppressive oligodeoxynucleotides inhibit silica-induced pulmonary inflammation. J Immunol. 2008; 180(11):7648–54. [PubMed: 18490767]
21. Devalaraja RM, Nanney LB, Du J, Qian Q, Yu Y, Devalaraja MN, Richmond A. Delayed wound healing in CXCR2 knockout mice. J Invest Dermatol. 2000; 115(2):234–44. [PubMed: 10951241]
22. Ishida Y, Gao JL, Murphy PM. Chemokine receptor CX3CR1 mediates skin wound healing by promoting macrophage and fibroblast accumulation and function. J Immunol. 2008; 180(1):569–79. [PubMed: 18097059]
23. Sato T, Takeno M, Honma K, Yamauchi H, Saito Y, Sasaki T, Morikubo H, Nagashima Y, Takagi S, Yamanaka K, Kaneko T, Ishigatsubo Y. Heme oxygenase-1, a potential biomarker of chronic silicosis, attenuates silica-induced lung injury. Am J Respir Crit Care Med. 2006; 174(8):906–14. [PubMed: 16858012]
24. Gerharz M, Baranowsky A, Siebolts U, Eming S, Nischt R, Krieg T, Wickenhauser C. Morphometric analysis of murine skin wound healing: standardization of experimental procedures and impact of an advanced multitissue array technique. Wound Repair Regen. 2007; 15(1):105–12. [PubMed: 17244326]
25. Kleinman HK, McGarvey ML, Hassell JR, Star VL, Cannon FB, Laurie GW, Martin GR. Basement membrane complexes with biological activity. Biochemistry. 1986; 25(2):312–8. [PubMed: 2937447]
26. Pfeffer U, Bisacchi D, Morini M, Benelli R, Minghelli S, Vacca A, Noonan DM, Albini A. Human chorionic gonadotropin inhibits Kaposi's sarcoma associated angiogenesis, matrix metalloprotease activity, and tumor growth. Endocrin. 2002; 143(8):3114–21.
27. Gorelik JV, Paramonov BA, Blinova MI, Diakonov IA, Kukhareva LV, Pinaev GP. Matrigel increases the rate of split wound healing and promotes keratinocyte utake' in deep wounds in rats. Cytotechnology. 2000; 32(2):79–86. [PubMed: 19002969]
28. Klaschik S, Gursel I, Klinman DM. CpG-mediated changes in gene expression in murine spleen cells identified by microarray analysis. Mol Immunol. 2007; 44(6):1095–104. [PubMed: 16930709]
29. Ishida Y, Gao JL, Murphy PM. Chemokine receptor CX3CR1 mediates skin wound healing by promoting macrophage and fibroblast accumulation and function. J Immunol. 2008; 180(1):569–79. [PubMed: 18097059]
30. Sester DP, Brion K, Trieu A, Goodridge HS, Roberts TL, Dunn J, Hume DA, Stacey KJ, Sweet MJ. CpG DNA activates survival in murine macrophages through TLR9 and the phosphatidylinositol 3-kinase-Akt pathway. J Immunol. 2006; 177(7):4473–80. [PubMed: 16982883]
31. Galiano RD, Tepper OM, Pelo CR, Bhatt KA, Callaghan M, Bastidas N, Bunting S, Steinmetz HG, Gurtner GC. Topical vascular endothelial growth factor accelerates diabetic wound healing through increased angiogenesis and by mobilizing and recruiting bone marrow-derived cells. Am J Pathol. 2004; 164(6):1935–47. [PubMed: 15161630]

32. Koff JL, Shao MX, Kim S, Ueki IF, Nadel JA. Pseudomonas lipopolysaccharide accelerates wound repair via activation of a novel epithelial cell signaling cascade. J Immunol. 2006; 177(12):8693–700. [PubMed: 17142770]

33. Fujimoto C, Klinman DM, yin H, Vistica BP, Wawrousek EF, Igarashi T, Chan C, Gery I. A suppressive oligodeoxynucleotide inhibits ocular inflammation. Clin Immunol Immunolpathol. 2009; l156(3):528–34.

34. Dorn A, Ludwig RJ, Bock A, Thaci D, Hardt K, Bereiter-Hahn J, Kaufmann R, Bernd A, Kippenberger S. Oligonucleotides suppress IL-8 in skin keratinocytes in vitro and offer anti-inflammatory properties in vivo. J Invest Dermatol. 2007; 127(4):846–54. [PubMed: 17139269]

35. Krieg AM. Therapeutic potential of Toll-like receptor 9 activation. Nat Rev Drug Discov. 2006; 5(6):471–84. [PubMed: 16763660]

36. Verthelyi D, Kenney RT, Seder RA, Gam AA, Friedag B, Klinman DM. CpG oligodeoxynucleotides as vaccine adjuvants in primates. J Immunol. 2002; 168(4):1659–63. [PubMed: 11823494]

37. Manegold C, Gravenor D, Woytowitz D, Mezger J, Hirsh V, Albert G, Al-Adhami M, Readett D, Krieg AM, Leichman CG. Randomized phase II trial of a toll-like receptor 9 agonist oligodeoxynucleotide, PF-3512676, in combination with first-line taxane plus platinum chemotherapy for advanced-stage non-small-cell lung cancer. J Clin Oncol. 2008; 26(24):3979–86. [PubMed: 18711188]

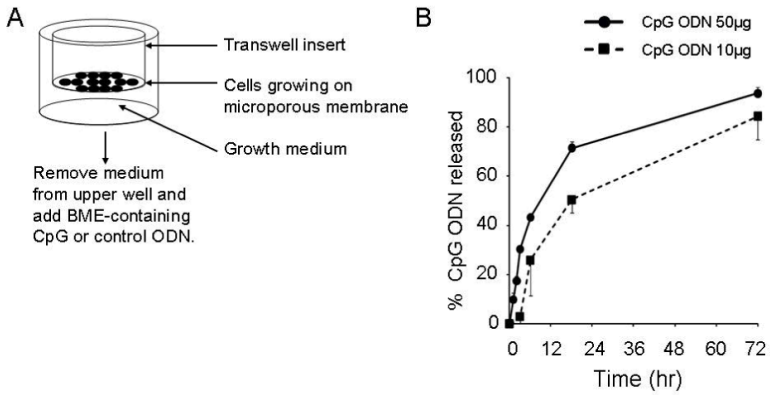

Figure 1. Release of CpG ODN formulated in basement membrane extract

A) Cells were grown to confluence on the 0.4 μm PVDF-coated membrane of a transwell insert. Culture medium was removed from the upper chamber and replaced with BME formulated with ODN. This mixture solidifies at 37° C. B) The kinetics of CpG ODN release from the BME was monitored by sampling medium from the lower chamber of the transwell plate over time. ODN concentration was monitored spectrophotometrically. Results reflect the avg + SD of 3 independent experiments.

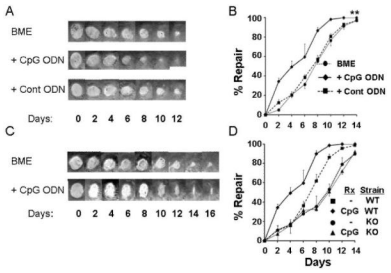

Figure 2. Effect of CpG ODN treatment on wound healing

Six mm excisional biopsies were taken from the right and left dorsum of individual mice. One biopsy site (selected at random) was treated on days 0, 2 and 4 with BME alone while the other was treated with BME formulated with 50 μg of either CpG or control ODN. Serial photographs of representative biopsy sites from (A) normal BALB/c and (C) congenic TLR9 KO mice are shown. B, D) The mean rate of repair was calculated based on the original wound area of each biopsy site. The percent repair over time (mean ± SE of all sites, N = 6/ treatment group from 2 independent experiments) is shown.

**; $p < 0.001$ for integrated area under the curve of BME + CpG ODN vs BME alone.

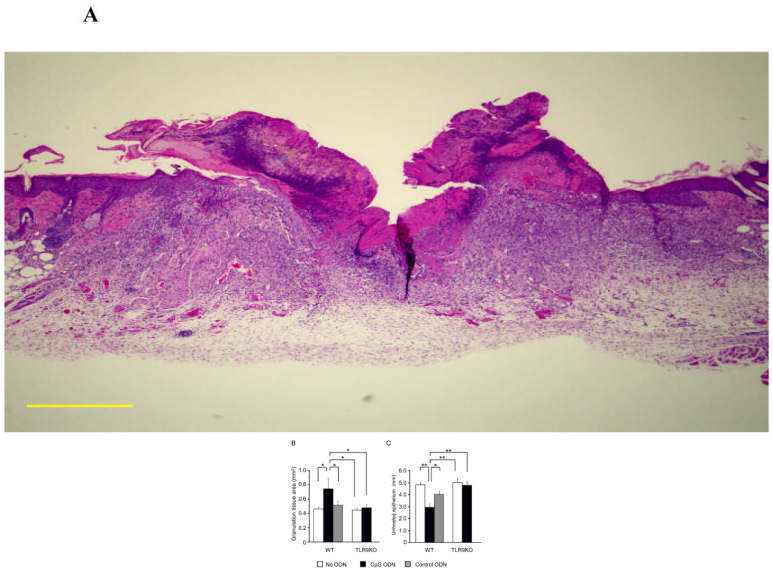

Figure 3. Effect of CpG ODN treatment on granulation tissue formation and re-epithelialization

BALB/c mice were treated as described in Fig 2. Serial sections were obtained from each biopsy site on day 4 (when the difference between treatment groups was greatest), stained with H & E, and the largest section analyzed morphometrically. (A) Representative photomicrograph of the wound bed identifying granulation tissue (G) and epidermal migration tongues (▼, original magnification 20X). Image J software was used to quantify the total area of granulation tissue (B) and the extent of re-epithelialization (the distance between epidermal migration tongues). Results represent the mean + SE of 2-3 independent experiments with 3 - 6 animals/group.

*, $p < 0.05$ and **, $p < 0.01$.

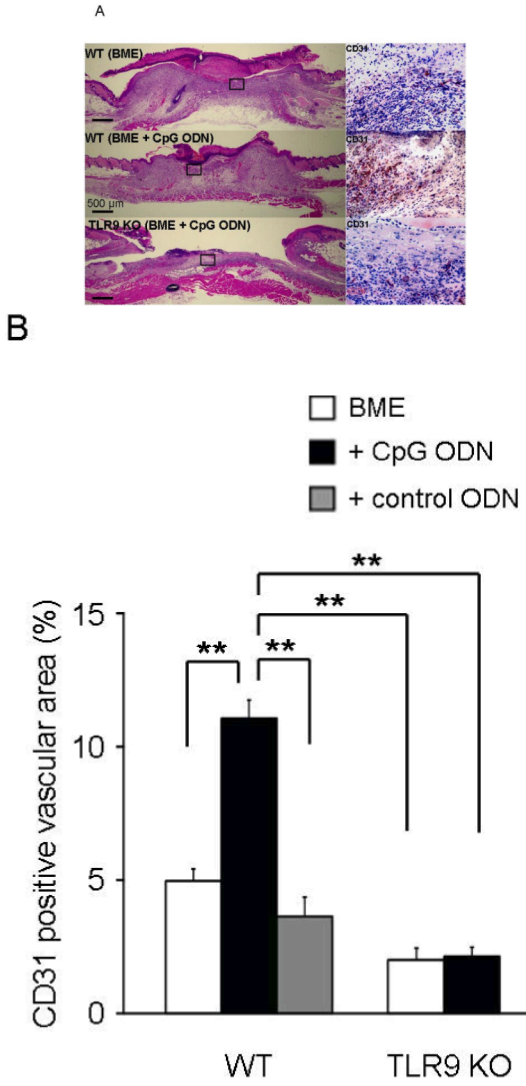

Figure 4. CpG ODN accelerate neovascularization of biopsy sites

Histologic sections were obtained from biopsy sites as described in Fig 3. (A) Photomicrographs of representative wild type (upper and middle panels) and TLR9 KO mice (lower panel; original magnification 20X). The insets show higher magnifications (400X) of CD31-stained sections of granulation tissue. (B) The re-vascularized area was calculated based on CD31 staining of representative tissue sections using Image J. Results represent the mean + SE of 2-3 independent experiments with 4-7 animals/group. **, $p < 0.01$.

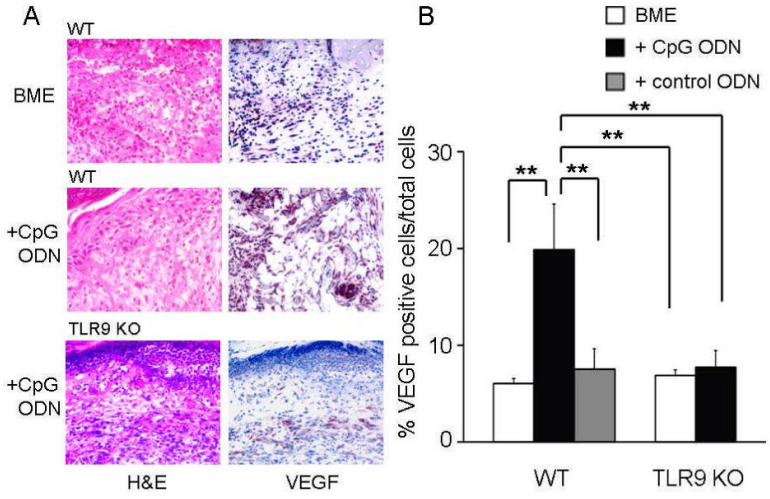

Figure 5. Effect of CpG treatment on VEGF expression at biopsy sites

Histologic sections were obtained from biopsy sites as described in Fig 3. (A) Photomicrographs from representative wild type mice (upper and middle panel) and TLR9 KO mice (lower panel, original magnification 400X) stained with anti-VEGF. (B) Percentage of $VEGF^{+}$ cells determined using Image J. Results represent the mean ± SE of 2-3 independent experiments with 4 - 8 animals/ group.

**, $p < 0.01$.

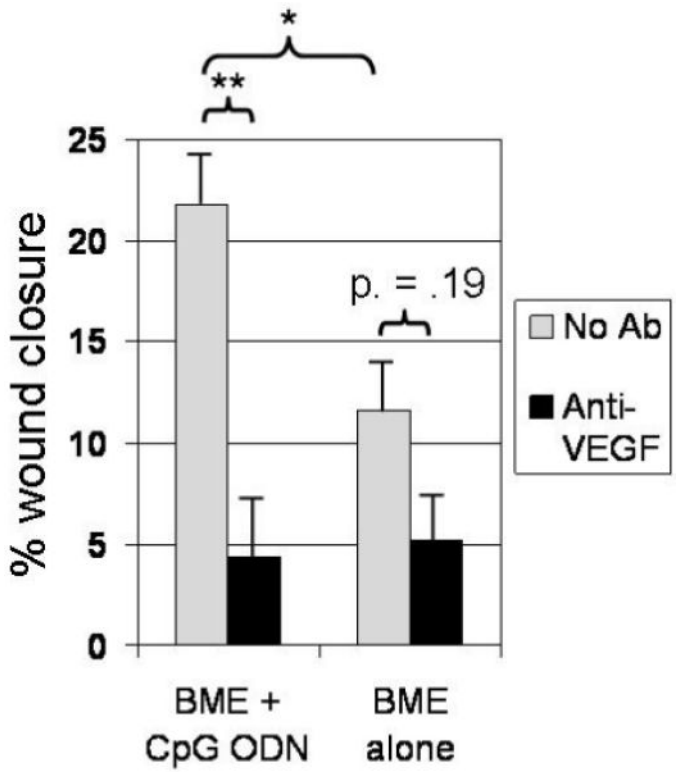

Figure 6. Neutralizing anti-VEGF Ab inhibits CpG-dependent acceleration of wound healing

BALB/c mice were injected i.p. with either PBS or anti-VEGF Ab on day -7, and re-injected 2x/wk. On day 0, 6 mm excisional biopsies were taken from the right and left dorsum of individual mice. One biopsy site (selected at random) was treated on days 0, 2 and 4 with BME alone while the other was treated with BME formulated with 50 μg of CpG ODN. The rate of wound healing on day 4 was analyzed as described in Fig 2. Results represent the mean ± SE of 2 independent experiments involving a total of 8 mice/group.
*; $p < 0.05$ and **; $p < 0.01$ for integrated wound area.

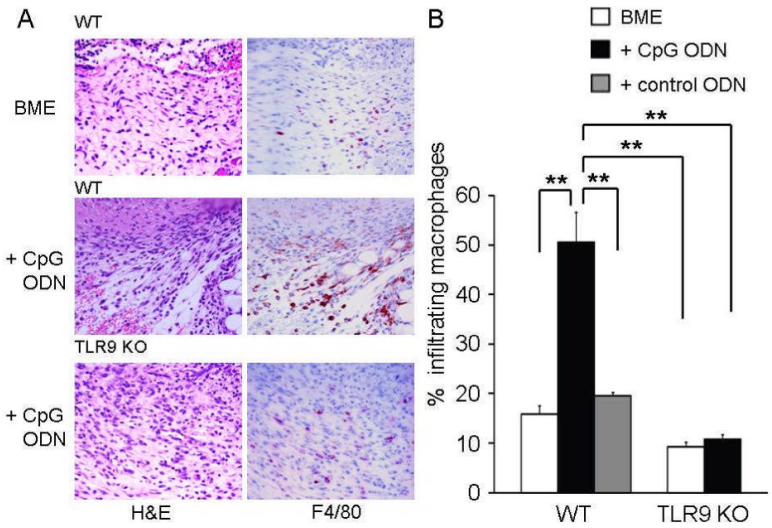

Figure 7. Histologic analysis of biopsy sites

Histologic sections were obtained from biopsy sites as described in Fig 3. (A) Photomicrographs from representative wild type mice (upper and middle panels) and TLR9 KO mice (lower panel, original magnification 400X) stained with H & E (left side) or anti-F4/80 (right side). (B) Macrophages as a percentage of the total number of infiltrating cells (mean + SE) from 3 independent experiments involving 3-4 animals/group.
**; $p < 0.01$

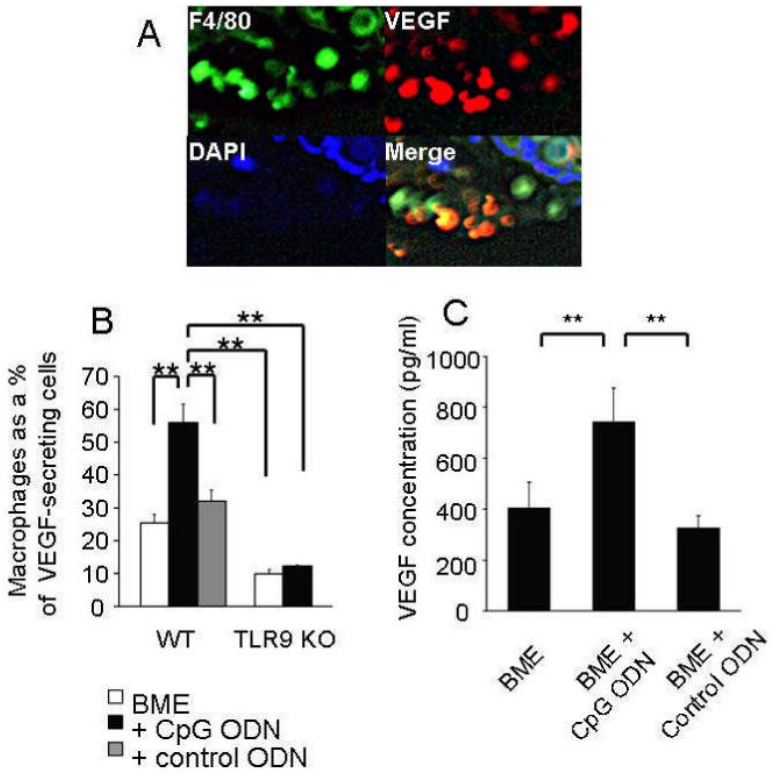

Figure 8. CpG ODN stimulate macrophages to produce VEGF

Histologic sections were obtained from biopsy sites as described in Fig 3. These were double stained with anti-F4/80 and anti-VEGF. A representative sample is shown in (A), and the mean + SE of VEGF secreting cells that were macrophages is shown in (B). Calculations based on 3 independent experiments involving histologic sections from 3 - 6 animals/group. (C) Freshly isolated peritoneal macrophages were cultured with BME ± 50 μg of CpG or control ODN. The concentration of VEGF protein in culture supernatants was examined on day 5 (the time point identified as optimal in preliminary experiments). Results represent the mean ± SE of 3 independent experiments.

**; $p < 0.01$.